Detection of Calibration Patterns for Camera Calibration with Irregular Lighting and Complicated Backgrounds

Dong-Joong Kang, Jong-Eun Ha, and Mun-Ho Jeong

Abstract: This paper proposes a method to detect calibration patterns for accurate camera calibration under complicated backgrounds and uneven lighting conditions of industrial fields. Required to measure object dimensions, the preprocessing of camera calibration must be able to extract calibration points from a calibration pattern. However, industrial fields for visual inspection rarely provide the proper lighting conditions for camera calibration of a measurement system. In this paper, a probabilistic criterion is proposed to detect a local set of calibration points, which would guide the extraction of other calibration points in a cluttered background under irregular lighting conditions. If only a local part of the calibration pattern can be seen, input data can be extracted for camera calibration. In an experiment using real images, we verified that the method can be applied to camera calibration for poor quality images obtained under uneven illumination and cluttered background.

Keywords: Camera calibration, detection of calibration pattern, length measurement system, machine vision, uneven illumination.

1. INTRODUCTION

Measurement of the dimensions of objects and parts in many industrial fields is very important, as the quality of the product depends especially on the reliability and precision of each object part. Popular sensor types for non-contact length measurements includes Moire, laser, and camera sensors, but measurement systems that utilize a camera are frequently used because they are inexpensive, easy to install, fast, and sufficiently accurate. In such systems, the calibration of the camera is essential because the images taken by the camera is used to measure dimensions of the object. The camera calibration is performed by modeling the optical projection through the camera lens and the relative locations between the object and camera in 3D space. Well-known methods of camera calibration include the Tsai [1] and Zhang [2] algorithms. With these methods, a known set of 3D points on a plane is projected to an image plane as input data and these points, known as a calibration pattern or as calibration points, are used to estimate the parameters of the camera.

Many studies on the subject of camera calibration [1-4] have focused on the estimation of camera parameters. However, the importance of data acquisition and matching steps has often been ignored in conventional research on camera calibration. Consequently, the difficulty of robust feature extraction and easy matching prevents the practical use of these methods.

The Tsai method of camera calibration uses the precise patterns marked on single or multiple planes and requires correspondence information between the 3D coordinates of the calibration pattern and their image coordinates to solve the internal and external parameters of the camera. Because this paper focuses on the measurement of objects located on a plane, we use the planar calibration method of the Tsai algorithm, which provides relatively easy and fast results with a single calibration pattern plane [1]. This calibration method requires at least seven calibration points of known positions to define all of the required camera parameters. The method was verified as the most exact calibration algorithm, based on the comparison tests by Salvi [3]. The method proposed

Manuscript received August 7, 2007; revised April 9, 2008; accepted May 22, 2008. Recommended by Editor Jae-Bok Song. This research was financially supported by the Ministry of Education, Science Technology (MEST) and Korea Industrial Technology Foundation (KOTEF) through the Human Resource Training Project for Regional Innovation. This work is financially supported by the Ministry of Education and Human Resources Development(MOE), the Ministry of Commerce, Industry and Energy(MOCIE) and the Ministry of Labor(MOLAB) through the fostering project of the Industrial-Academic Cooperation Centered University.

Dong-Joong Kang is with the School of Mechanical Engineering, Pusan National University, 30 Jangjeon-dong, Geumjeong-gu, Busan 609-735, Korea (e-mail: djkang@pusan.ac.kr).

Jong-Eun Ha is with the Dept. of Automotive Engineering, Seoul Nat. Univ. of Tech., 172 Gongreung, Nowon-gu, Seoul, Korea (e-mail: jeha@snut.ac.kr).

Mun-Ho Jeong is with Intelligent Robotics Center, KIST, 39 Hawolgok-dong, Seongbuk-gu, Seoul, Korea (e-mail: jeong.kist@gmail.com).

by Zhang [2] is very easy to use and provides relatively good calibration parameters. However, the method requires 10~20 images of a calibration pattern that are located on the planes of different pose and hence, the method is not adequate to apply in industrial fields for length measurement.

Usually, lighting conditions in industrial settings are not well controlled for precise and easy calibration of a camera. It is difficult to expect accurate camera calibration under such illumination conditions, as the lighting condition hinders the exact extraction of the calibration pattern.

This paper proposes a data selection method to overcome these limitations. A probabilistic criterion is proposed to detect a local set of calibration points, which would guide the extraction of other calibration points under cluttered backgrounds and irregular lighting conditions. A plane-to-plane transformation is used to determine the one-to-one point correspondence between calibration patterns and their projection on the image plane. The coordinates of the extracted initial points are used as input data for the nonlinear optimization of Tsai calibration, and the internal and external parameters that result from the calibration are used again to extract the points for which the distance error between the image points and projected points of the calibration pattern fall within error allowances after world-to-image transformation by Tsai calibration parameters. As a result, additional calibration points are added to recalculate the calibration method. Using this procedure, the calibration method becomes sufficient to extract precise camera parameters. This method can be used in factories where lighting conditions are difficult to control. The method was tested in experiments using real images from irregular lighting conditions with complicated backgrounds.

(a) A sample part known as a door-belt that is one of car component.

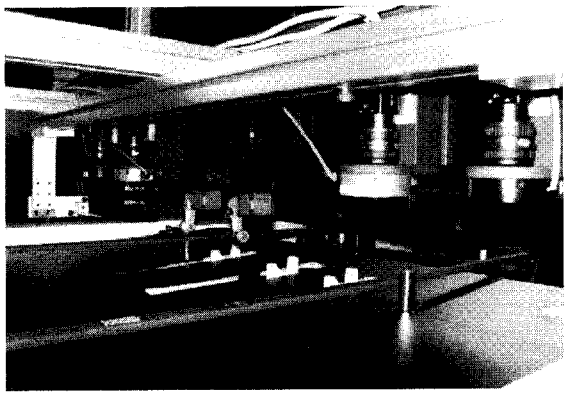

(b) Visual inspection system equipped with LED lamps and inspection cameras.

Fig. 1. Measurement of a mechanical part by the machine vision system (Courtesy of Sedong Corp).

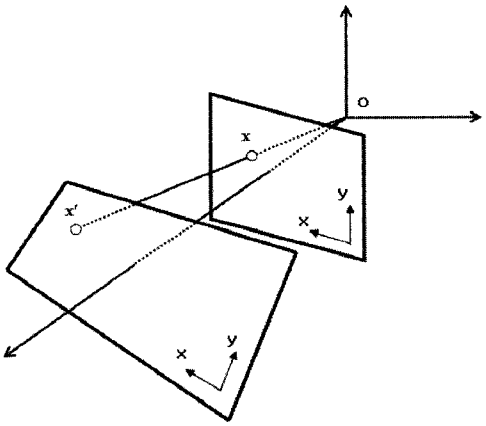

Fig. 2. Plane projective transformation.

2. DETECTION OF CALIBRATION PATTERN

2.1. Plane-to-plane mapping

Fig. 1(a) shows a sample of the mechanical part that requires measurement of the object dimension. The visual inspection system shown in Fig. 1(b) is equipped with four machine-vision cameras with pre-calibrated parameters. Light-emitting diode (LED) lamps are attached to control the lighting condition of the inspection sample. This inspection machine was designed to measure objects with long lengths, as it can observe a wide range of an object by using multiple cameras.

The Tsai calibration requires over seven calibration points and requires users to enter the exact coordinates of the points and one-to-one matching information between calibration points of an image and their world coordinates. This preparation of data becomes a difficult and very inconvenient procedure if the image projection of a pattern for camera calibration contains interference due to poor lighting conditions.

This paper uses perspective transformation of a plane to extract point coordinates for calibration. A simple perspective projection is a plane-to-plane mapping, as shown in Fig. 2, which does not include lens distortion. Thus, it is not appropriate for camera calibration. However, because four calibration points can create a projection matrix of a plane, it can be applied to predict the input points of the calibration.

$$s\mathbf{x} = s\begin{bmatrix} x \\ y \\ 1 \end{bmatrix} = \mathbf{H}\mathbf{x}' = \begin{bmatrix} h_{11} & h_{12} & h_{13} \\ h_{21} & h_{22} & h_{23} \\ h_{31} & h_{32} & h_{33} \end{bmatrix}\begin{bmatrix} x' \\ y' \\ 1 \end{bmatrix} \quad (1)$$

Equation (1) shows the relationship between world coordinates $\mathbf{x}'$ of 3D points on a calibration pattern plane and calibration coordinates $\mathbf{x}$ on an image plane transformed by homography matrix $\mathbf{H}$ [5,6]. The value s is a scale factor, and $h_{33}=1$ represents a constraint to limit the magnitude of the elements of the homography matrix. Equation (1) is as follows:

$$\begin{aligned} x(h_{31}x'+h_{32}y'+1) &= h_{11}x'+h_{12}y'+h_{13}, \\ y(h_{31}x'+h_{32}y'+1) &= h_{21}x'+h_{22}y'+h_{23}. \end{aligned} \tag{2}$$

$$\begin{bmatrix} x' & y' & 1 & 0 & 0 & 0 & -xx' & -xy' \\ 0 & 0 & 0 & x' & y' & 1 & -yx' & -yy' \end{bmatrix} \begin{bmatrix} h_{11} \\ h_{12} \\ h_{13} \\ h_{21} \\ h_{22} \\ h_{23} \\ h_{31} \\ h_{32} \end{bmatrix} = \begin{bmatrix} x \\ y \end{bmatrix}. \tag{3}$$

Using the pseudo-inverse formula of (3) if more than four points exist, it is possible to determine $h_{11} \sim h_{32}$ for the plane projection transformation.

Once the homography matrix is determined, the world coordinates on the calibration pattern can be projected onto the image plane. Points with small distance errors between the pattern points and their projections on the image plane can then be used for the nonlinear optimization of the calibration algorithm.

2.2. Extraction of noise free points

An image sample of a calibration pattern acquired from a camera is shown in Fig. 3. Tuning lights such as an LED or a halogen lamp to obtain uniform intensity on the calibration pattern is not easy under the dynamic illumination conditions in factories. The image is binarized to intensity values of 0 and 255, as shown in Fig. 3(b), and then pixels of intensity value 255 are labeled to point regions [7]. The Otzu method can be used to select the threshold value for the automatic binarization of the gray-scale image [8,9]. The method provides an optimal threshold constant for the minimization of the probabilistic variance for two normal distributions of the background and object in the image region. The labeled areas are mixed with noisy regions and accurate calibration points, as shown in Fig. 3(b). The calibration points of the areas marked with an ellipse in Fig. 3(b) are on the regions where the intensity value is similar to the threshold value for binarization. Because the boundaries of the calibration points can include the background regions that make the center position of the regions to shift and distort, the points of an unclear boundary should be discarded to select the correct candidate points for use in the calibration of a camera.

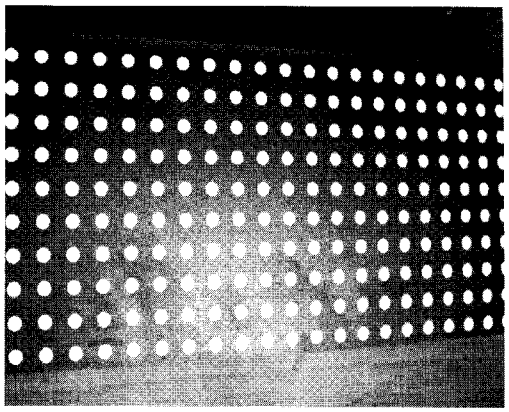

(a) Original gray image.

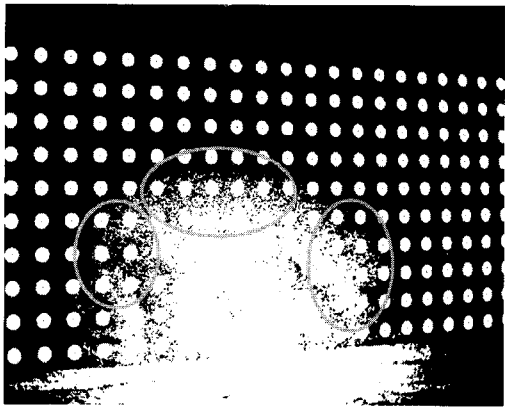

(b) Segmented points by Otzu binarization. Areas marked with an ellipse include noisy regions.

Fig. 3. Extraction of calibration points.

To select noise-free calibration points and solve the matching problem between world points on the calibration pattern and their projections on an image plane, a *cross pattern of five points* on an image plane is extracted, as shown in Fig. 4(a). Among all the blob regions remaining after the elimination of excessively small and large regions, the four neighborhood points closest to the center position of each blob are chosen.

The cross-type pattern is a projection of a set of a small number of points on the calibration pattern. The origin of the coordinate system can be assumed as always being located at the center point of the set, as shown in Fig. 4(b). The four reference points of the cross pattern are at similar distances from the center point of the cross pattern.

Because the line $x_1'x_2'$ on the calibration pattern is parallel to the line $x_2'x_3'$, the cross pattern on the image plane including the noise-free calibration points has to satisfy the condition in which lines l_1 and l_2 are parallel to lines l_3 and l_4, respectively. If a projection of a calibration point on the image plane is contaminated by image noise, the distortion of the center position in the region then affects the parallel relationship of the two lines.

A probabilistic criterion can be provided to select a

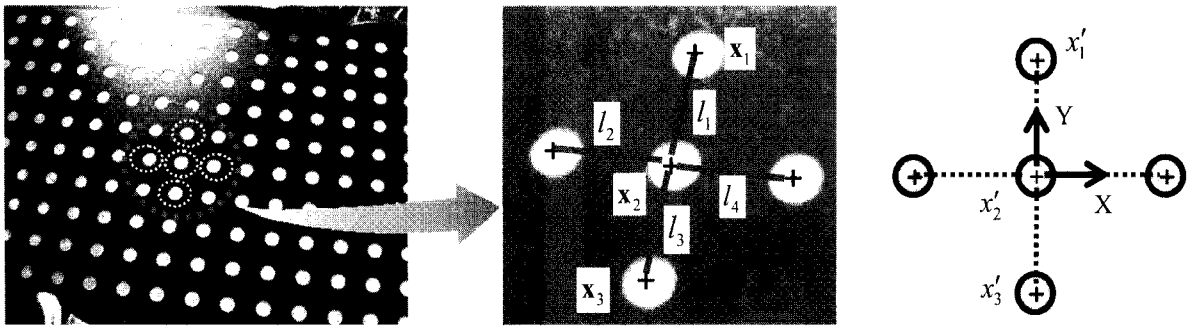

(a) (b)

Fig. 4. A set of five calibration points: (a) Five points on an image plane. (b) Reference points with respect to the coordinate system of the calibration pattern.

set of noise-free points in a noisy binary image. The parallelism between two lines in Fig. 4(a) is defined as a function of six variables:

$$f = \cos^{-1}\left(\frac{\mathbf{a}\cdot\mathbf{b}}{|\mathbf{a}||\mathbf{b}|}\right), \tag{8}$$

where $\mathbf{a} = \mathbf{x}_2 - \mathbf{x}_1$ and $\mathbf{b} = \mathbf{x}_3 - \mathbf{x}_2$

or $f = f(\mathbf{x}_1, \mathbf{x}_2, \mathbf{x}_3)$, where $\mathbf{x}_i = (x_i, y_i, 1)^T$. (9)

$\mathbf{x}_i (i = 1,...3)$ denotes the image coordinates for the endpoints of the two lines, and $|\mathbf{a}|$ represents the length of vector $\mathbf{a}$. To avoid using a trigonometric function in the calculation of the partial derivatives of function f with respect to the image coordinates, a simpler function is used:

$$f' = \cos(f) = \frac{\mathbf{a}\cdot\mathbf{b}}{|\mathbf{a}||\mathbf{b}|} = f'(\mathbf{x}_1, \mathbf{x}_2, \mathbf{x}_3). \tag{10}$$

If (x_i, y_i) are true and $(\tilde{x}_i, \tilde{y}_i)$ the noisy observation of (x_i, y_i), the following results:

$$\tilde{x}_i = x_i + \xi_i, \tag{11a}$$

$$\tilde{y}_i = y_i + \eta_i. \tag{11b}$$

where the noise terms ξ_i and η_i denote independently the distributed noise terms having a mean of 0 and variance of σ_i^2. Hence,

$$\mathrm{E}[\xi_i] = \mathrm{E}[\eta_i] = 0, \tag{12}$$

$$\mathrm{V}[\xi_i] = \mathrm{V}[\eta_i] = \sigma_i^2, \tag{13}$$

$$\mathrm{E}[\xi_i \xi_j] = \begin{cases} \sigma_0^2 & \text{if } i = j \\ 0 & \text{otherwise,} \end{cases} \tag{14a}$$

$$\mathrm{E}[\eta_i \eta_j] = \begin{cases} \sigma_0^2 & \text{if } i = j \\ 0 & \text{otherwise,} \end{cases}$$

$$\mathrm{E}[\xi_i \eta_j] = 0. \tag{14b}$$

From these noisy measurements, the noisy parallel function is defined:

$$\tilde{f}'(\tilde{x}_1, \tilde{y}_1, \tilde{x}_2, \tilde{y}_2, \tilde{x}_3, \tilde{y}_3). \tag{15}$$

To determine the expected value and variance of $\tilde{f}'$, $\tilde{f}'$ is expanded as a Taylor series at $(x_1, y_1, x_2, y_2, x_3, y_3)$:

$$\begin{aligned} \tilde{f}' &\approx f' + \sum_{i=1}^{3}\left[(\tilde{x}_i - x_i)\frac{\partial \tilde{f}'}{\partial \tilde{x}_i} + (\tilde{y}_i - y_i)\frac{\partial \tilde{f}'}{\partial \tilde{y}_i}\right] \\ &= f' + \sum_{i=1}^{3}\left[\xi_i \frac{\partial \tilde{f}'}{\partial \tilde{x}_i} + \eta_i \frac{\partial \tilde{f}'}{\partial \tilde{y}_i}\right]. \end{aligned} \tag{16}$$

The variance of the parallel function then becomes

$$\begin{aligned} \mathrm{Var}(f') &= E\left[(\tilde{f}' - f')^2\right] \\ &= \sigma_0^2 \sum_{i=1}^{3}\left[\left(\frac{\partial \tilde{f}'}{\partial \tilde{x}_i}\right)^2 + \left(\frac{\partial \tilde{f}'}{\partial \tilde{y}_i}\right)^2\right]. \end{aligned} \tag{17}$$

Hence, for two given lines, a threshold can be determined as:

$$\Delta f = 3 \cdot \sqrt{E[(\tilde{f}' - f')^2]}. \tag{18}$$

As the optimal f' equals 1, any two parallel lines have to satisfy the following condition:

$$1 - \tilde{f}' \le \Delta f. \tag{19}$$

If the line pair (l_1, l_3) or (l_2, l_4) do not satisfy the condition of (19), the cross pattern of five points will not be accepted as a set of noise-free calibration points on the image plane. After the five point set passes the probabilistic criterion, the cross pattern is then used to solve the homography matrix of (3) and guide other points on the calibration pattern into positions of blob points on the image plane.

2.3. Decision of calibration points

The five point group of Fig. 4(b) has a symmetric form of four other points with respect to the center point of the set, and the correspondence problem between the image points and reference points on the calibration pattern can be solved simply by extracting the equivalent pattern for blob points on the image plane.

Although the projected circle center differs from the ellipse centers, as mentioned in [4,10], the calibration pattern in this paper is a small circle and very similar to the shape of a circle under even severe perspective projection. Because the direction of the axis of the camera in a length measurement system is typically similar to the normal direction of the calibration pattern plane, the position of the ellipse center can be used as the center of the calibration point.

After the probabilistic test of Section 2.2 for the cross patterns of five points, several cross pattern groups can be accepted, and the most probable group is selected. For the homography matrix calculated from each cross pattern of five points, the reference points on the calibration pattern can be transformed into coordinates of the image plane, and the error distances between the projection of the reference points and image coordinates of their corresponding blob regions can be checked. Because outliers always exist by noisy binary points even when only small groups pass the probabilistic test, indicating that some distance errors between the corresponding points from the plane-to-plane transformation may be large, the median value of the errors can be chosen to reject the point group with outliers. All distance errors from each point are sorted and the median value of the error magnitude is selected as the threshold t_m.

Given that a five-point homography matrix can guide the plane transformation of other points on a calibration pattern, the points close to the five point group on the calibration pattern can also be transformed to the image plane. $10t_m(=th_1)$ was set as the threshold of the distance error to reject or accept the corresponding points after transformation for neighboring points of the cross pattern.

Among all candidates that passed the probabilistic criterion of (19), a cross pattern with the homography matrix that provides the largest corresponding pairs in the permitted range th_1 was chosen as the point group of an optimal plane-to-plane transformation. Their corresponding point pairs were also selected as the initial data of the calibration algorithm.

2.4. Camera calibration

The homography matrix represents only the plane-to-plane mapping relationship. Lens distortion in the camera system is irrelevant in this matrix. Therefore, distance error between the image and the projected points always exists, specifically in the image boundary area due to the radial distortion of the camera lens.

If the re-projection error after the camera calibration considering the radial distortion is smaller than the allowance of the distance error between the image and projected points, the algorithm ends. If not, the internal and external parameters after the calibration are used to project the points of the calibration pattern onto the image plane again. Because the Tsai calibration considers the radial distortion of the camera lens, the coordinates of the projected points approach the position of the labeled points of the image, implying that additional calibration points smaller than th_1 can be extracted. The extracted coordinates of the additional points can be used to execute the calibration procedure again until the number of incoming points does not increase. Although poor illumination and complicated backgrounds cause interference, accurate camera calibration results can be achieved.

Fig. 5 shows the entire procedure of the proposed algorithm to detect the calibration pattern and execute camera calibration by Tsai method. The main body of algorithm is repetitive adding of new calibration points through the evaluation of the distant error between the calibration target points and their image projection by use of calibration parameters such as the lens distortion coefficient and focal length.

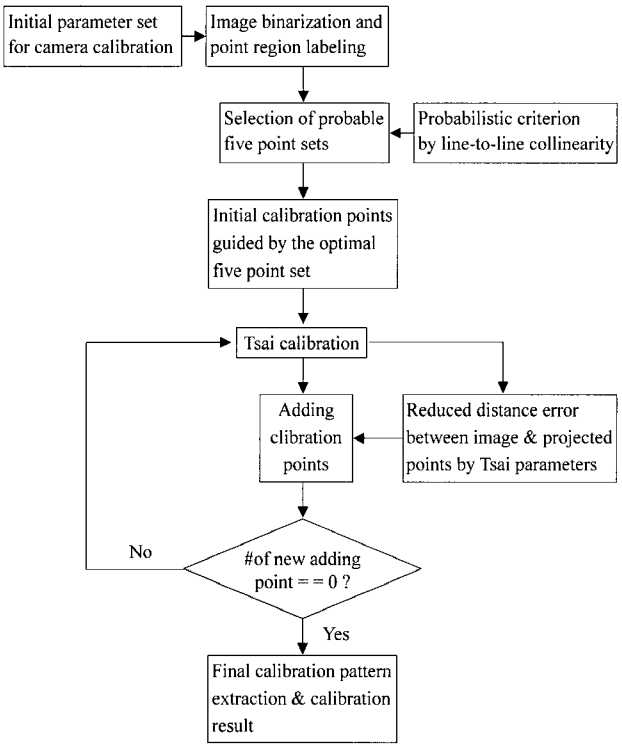

Fig. 5. Procedure of calibration pattern detection algorithm.

3. EXPERIMENTS

The experiments utilized a Matrox Meteor II frame grabber and a Sony XC-75 camera for image acquisitions. The camera calibration pattern consisted of round dots of 4.5mm in diameter, which were placed at a distance of 10mm covering 900mm x 100mm with white circle marks on a black background.

The proposed method was tested for patterns of different sizes under different backgrounds and uneven illumination. The image size was 640x480 pixels and the algorithm was implemented using C++ under Windows XP environment.

Fig. 6 shows the experimental result for the probabilistic test of Section 2.2. The original gray-scale image in Fig. 6(a) is binarized using the Otzu method, and the criterion of (19) verifies the parallelism of lines for five points of each cross pattern. When each parallel relationship of two lines created from five points satisfies the variance test, the five points of the cross pattern become a noise-free point set, and the center point of the cross pattern is marked with a rectangle, as shown in Fig. 6(b). All points marked with a rectangle are the center position of each of the five point set and have four neighboring points.

The original image of Fig. 6(a) includes irregular light reflections on the calibration pattern, and conventional techniques such as the use of a morphology filter or local adaptive image binarization can not eliminate the noisy regions extracted from the uncontrolled illumination. Noisy regions extracted from uncontrolled environments can shift and distort the center position of the calibration point and violate the parallel constraint between the lines of the cross pattern of five points.

Fig. 7 presents other images of the calibration pattern captured under conditions that included a cluttered background and uneven lighting. The sizes of the calibration points are relatively small and several noisy regions including the calibration points and background clutter are shown. The experimental result showed that the proposed probabilistic test extracted only correct calibration points. Heuristic parameters were unnecessary, and all steps of the algorithm were automatically performed for sample images without user intervention. In addition, a change in the illumination density on the calibration pattern plane did not affect the result. Although changes to the image scale including the calibration points were made by the change of the distance from the camera to the calibration pattern, the performance of the algorithm was not affected, as shown in the experimental results of Figs. 6 and 7.

Fig. 8 shows the distribution of the threshold values for several points in the first two images of Fig. 6 (large scale) and Fig. 7 (small scale). When the image scale was changed, the threshold value used to choose the parallel relationship also changed adaptively according to the changes in the size of the dots and their distance from each other. In the graph, std1 and std2 are the standard deviation values of (19) for the two parallel constraints of line pairs (l_1, l_3), (l_2, l_4) of Fig. 4, respectively.

Fig. 9 shows two calibration results by the Tsai method. First, the best five point set was determined to be the point set that resulted in the largest corresponding pairs from the homography test of Section 2.3 (the second column in the figure). Local

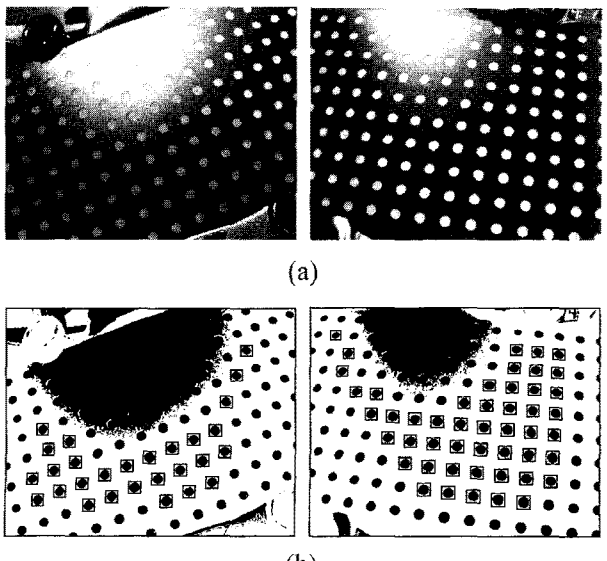

(a) (b)

Fig. 6. Extraction of a calibration pattern under uneven illumination.

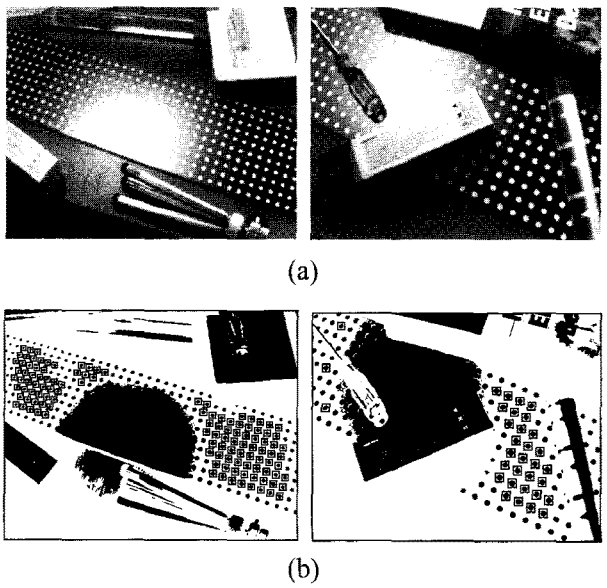

(a) (b)

Fig. 7. Extraction of a smaller calibration pattern with occlusion, irregular lighting, and complicated background.

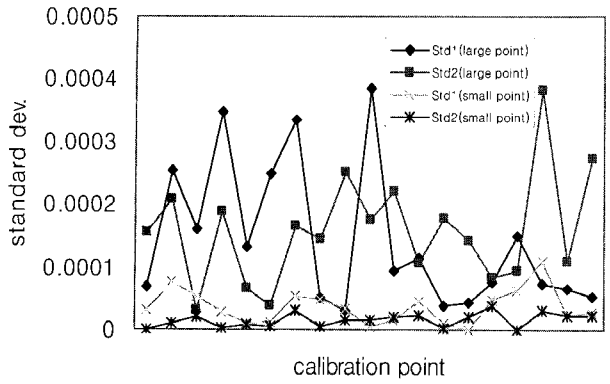

Fig. 8. Adaptive threshold value determining the co-linearity of the calibration points according to the change of the image scale.

neighborhood points smaller than th_1 were then selected from the homograph transformation. These points were used as input data for the Tsai calibration and the result of the calibration algorithm provided accurate values of camera parameters, considering the radial distortion.

More points were added during the repeated calibration based on the distance error between the calibration pattern and the image points. The images in the last column in Fig. 9 show the final extraction of the calibration points. All extractions are undistorted and noise-free points. The computation time for all procedures was approximately 1 sec using a Pentium-IV processor.

For the camera calibration, Table 1 shows the number of calibration points used during the iteration, the distortion coefficient of the lens, and the average distance error after repeated projections of the image points onto the calibration pattern using the camera parameters. Also, the focal length of Tsai calibration is presented with the number of the data point used for the calibration. Although many points were added to the calibration algorithm during the iteration process, the average distance error did not increase significantly, as the radial distortion coefficient of the camera lens and other calibration parameters changed to minimize the overall error level of the camera system. The input parameters of Tsai method were set as follows: 768 and 640 for the number of sensor elements in the X and Y directions; 320 and 240 for row and column numbers of the center of the computer frame memory; scale factor 1; and 0.0084, 0.0098 for center to center distance of camera's sensor element for X and Y direction, respectively.

Fig. 10 shows the result of the calibration pattern extraction under different illumination conditions for the same view of a fixed camera. The distance between the halogen ramp and calibration pattern plane was changed and accordingly, a few images were captured by a fixed camera. Even though there

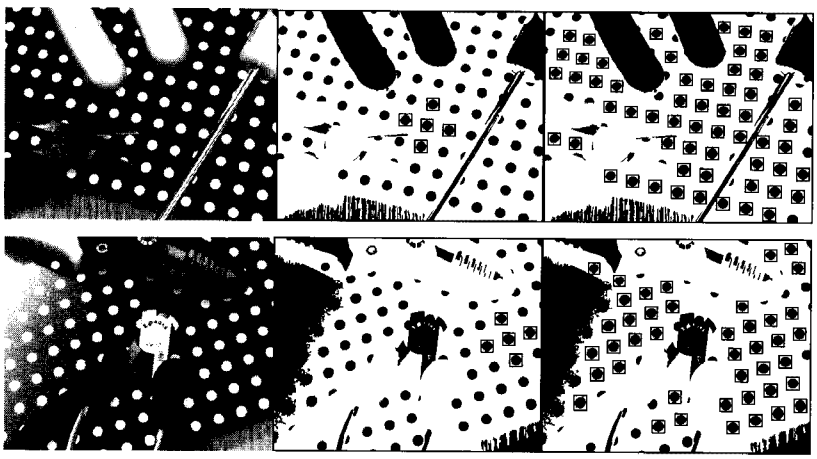

Fig. 9. Of the Tsai calibration. Original image, most probable point set, and final point extraction after repetition of Tsai calibration.

Table 1. Calibration results during iteration of the Tsai algorithm.

ITERATION		1	2	3	4	5
IMAGE 1 (1ST ROW)	# OF CALIBRATION POINTS	28	32	47	44	44
	DISTANCE ERROR (mm)	0.0345	0.0348	0.0621	0.0498	0.0498
	DISTORTION COEFF. ($1/mm^2$)	0.00185	0.00164	0.0012	0.00107	0.00107
	FOCAL LENGTH(mm)	16.2	16.1	17.2	17.5	17.5
IMAGE 2 (2ND ROW)	# OF CALIBRATION POINTS	9	12	15	15	15
	DISTANCE ERROR (mm)	0.0141	0.0161	0.0250	0.0250	0.0250
	DISTORTION COEFF. ($1/mm^2$)	0.00196	0.00174	0.00035	0.00034	0.00034
	FOCAL LENGTH(mm)	21.6	22.2	17.7	17.6	17.6

(a) Original images.

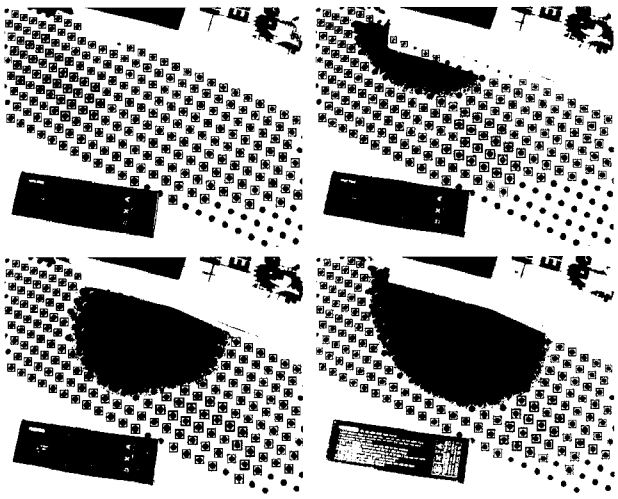

(b) Calibration pattern extraction.

Fig. 10. Calibration pattern extraction under different illumination conditions with a fixed camera.

was a severe change of light reflection, the calibration pattern could be extracted reliably. When the light source approaches the calibration plane, the number of calibration points that can be detected reduces and the position of detected points concentrates on the image side because the image center position has a strong light reflection. The background clutters created by a small box, a book, and characters on the book do not affect the extraction of the calibration points.

4. CONCLUSIONS

A robust recognition method of a calibration pattern for camera calibrations was presented in this paper. The method performs the extraction of a calibration pattern and a camera calibration using the planar pattern for accurate calibrations under conditions that include uneven illumination and complicated backgrounds. First, a probabilistic criterion detects a local set of calibration points among round dot patterns that are equally spaced, and this point set then guides the extraction of other calibration points. A homography transformation was used to test the correspondence between the image points and reference points on a calibration pattern. If any local part of the calibration pattern is observed, the extraction of input data is then considered possible for camera calibration. Experiments showed that the method was fast, easy to use, and robust for pattern images in cluttered backgrounds and irregular lighting conditions.

REFERENCES

[1] R. Tsai, "A versatile camera calibration technique for high-accuracy 3D machine vision metrology using off-the-shelf TV cameras and lenses," *IEEE Journal of Robotics and Automation*, vol. 3, no. 4, pp. 323-344, 1987.

[2] Z. Zhang, "A flexible new technique for camera calibration," *IEEE Trans. on Pattern Analysis and Machine Intelligence*, vol. 22, no. 11, pp. 1330-1334, Nov. 2000.

[3] J. Salvi, X. Armangue, and J. Batlle, "A comparative review of camera calibrating methods with accuracy evaluation," *Pattern Recognition*, vol. 35, no. 7, pp. 1617-1635, 2002.

[4] J. S. Kim, P. Gurdjos, and I. S. Kweon, "Geometric and algebraic constraints of projective concentric circles and their applications to camera calibration," *IEEE Trans. on Pattern Analysis and Machine Intelligence*, vol. 27, no. 4, pp. 637-642, 2005.

[5] O. Faugeras and Q. Luong, *The Geometry of Multiple Images*, MIT Press, 2001.

[6] E. Trucco, F. Isgrò, and F. Bracchi, "Plane detection in disparity space," *Proc. of the IEE International Conference on Visual Information Engineering*, Guildford, Surrey, UK, pp. 73-76, July 2003.

[7] I. Pitas, *Digital Image Processing Algorithms and Applications*, Wiley Inter-Science, 2000.

[8] N. Otsu, "A threshold selection method from gray-level histograms," *IEEE Trans. on Systems, Man, and Cybernetics*, vol. SMC-9, pp. 62-66, 1979.

[9] R. M. Haralick and L. G. Shapiro, *Computer and Robot Vision*, Addison Wesley, 1992.

[10] G. Jiang and L. Quan, "Detection of concentric circles for camera calibration," *Proc. of IEEE Int. Conf. on Computer Vision*, pp. 333-340, 2005.

Dong-Joong Kang received the B.S. degree in Precision Engineering from Pusan National University, Pusan, Korea, in 1988 and the M.E. degree in Mechanical Engineering from KAIST (Korea Advanced Institute of Science and Technology), Seoul, Korea, in 1990. He also received the Ph.D. degree in Automation and Design Engineering at KAIST, in 1998. In 1997-1999, he was a Research Engineer at SAIT (Samsung Advanced Institute of Technology). During 2000-2006, he was an Assistant Professor at the Department of Mechatronics Engineering in Tongmyong University. Since 2006, he has been an Assistant Professor at the School of Mechanical Engineering in Pusan National University. His current research interests are visual surveillance, intelligent vehicles, robotics, and machine vision.

Jong-Eun Ha received the B.S. and M.E. degrees in Mechanical Engineering from Seoul National University, Seoul, Korea, in 1992 and 1994, respectively, and the Ph.D. Degree in Robotics and Computer Vision Lab. at KAIST in 2000. During 2000. 2-2002. 8, he worked at Samsung Corning where he developed machine vision system. During 2002. 9-2005. 8, he was a Full-time Lecturer at the Department of Multimedia Engineering in Tongmyong University. Since 2005, he has been an Assistant Professor at the Department of Automotive Engineering in Seoul National University of Technology. His current research interests are intelligent vehicles/ robotics, object detection and recognition.

Mun-Ho Jeong is a Senior Research Scientist at the center for cognitive robotics research, Korea Institute of Science and Technology (KIST). He obtained the Ph.D. from the Department of Mechanical Engineering for Computer-controlled Systems, Osaka University, Japan. His major interests are computer/robot vision, image processing and human-robot interaction.